Editorial Manager(tm) for Materials Science and Technology
Manuscript Draft

Manuscript Number: MST9464R1

Title: Transition of amorphous to crystalline oxide film in initial oxide overgrowth on liquid metals

Article Type: Original Research Paper

Keywords: Thermodynamics; Oxidation; Liquid metal; Amorphous phase

Corresponding Author: Prof. ZHONGYUN FAN, Professor

Corresponding Author's Institution: Brunel University

First Author: Hua Men

Order of Authors: Hua Men; ZHONGYUN FAN, Professor

Abstract: It is important to understand the mechanism of oxidation in the initial stage at free surface on liquid metals. Mittemeijer and co-workers recently developed a thermodynamic model to study the oxide overgrowth on a solid metal surface. Based on this model, we have developed a thermodynamic model to analyze the thermodynamic stability of oxide overgrowth on liquid metals. The thermodynamic model calculation revealed that the amorphous oxide phase is thermodynamically preferred up to 1.3 and 0.35nm, respectively, in the initial oxide overgrowth on liquid Al and Ga at the corresponding melting point. However, the amorphous phase is thermodynamically unstable in the initial oxide overgrowth on liquid Mg. The thermodynamic stability of amorphous phase in the Al and Ga oxide systems is attributed to lower sums of surface and interfacial energies for amorphous phases, compared to that of the corresponding crystalline phases.

Transition of amorphous to crystalline oxide film in initial oxide overgrowth on liquid metals

H. Men, Z. Fan*

BCAST, Brunel University, Uxbridge, Middlesex UB8 3PH, UK

Abstract

It is important to understand the mechanism of oxidation in the initial stage at free surface on liquid metals. Mittemeijer and co-workers recently developed a thermodynamic model to study the oxide overgrowth on a solid metal surface. Based on this model, we have developed a thermodynamic model to analyze the thermodynamic stability of oxide overgrowth on liquid metals. The thermodynamic model calculation revealed that the amorphous oxide phase is thermodynamically preferred up to 1.3 and 0.35 nm, respectively, in the initial oxide overgrowth on liquid Al and Ga at the corresponding melting point. However, the amorphous phase is thermodynamically unstable in the initial oxide overgrowth on liquid Mg. The thermodynamic stability of amorphous phase in the Al and Ga oxide systems is attributed to lower sums of surface and interfacial energies for amorphous phases, compared to that of the corresponding crystalline phases.

Keywords: Thermodynamics; Oxidation; Liquid metal; Amorphous phase

1. Introduction

Research on oxidation at free surfaces of liquid metals (LMs) is of the fundamental and scientific interests. Oxide films easily form on the free surface of LMs even under high vacuum conditions, especially for reactive elements such as Al and Mg. For example, an atomic scale oxide-free aluminum surface in thermodynamic equilibrium is impossible because the maximum oxygen partial pressure that is in equilibrium with physically dissolved oxygen is 10^{-40} bar.[1] Surface oxidation of LMs can dramatically change the surface tension which will have a significant effect on the way LMs wet different surfaces.[2,3] This is important for the process, such as soldering, brazing, casting and so on. There are considerable differences between the ways

* Corresponding author. Tel.: +44 1895 266406; fax: +44 1895 269758.
E-mail address: Zhongyun.Fan@brunel.ac.uk (Z. Fan).

oxidation develops in various LMs. For example, the formation of a relatively thin surface oxide layer (e.g. an Al_2O_3 oxide film at the surface of liquid Al) effectively prevents the bulk from further oxidation to reduce melt losses (2~10% for Al alloys) during melting.[4] On the other hand, oxidation of liquid Mg produces a discontinuous oxide film.[5]

It has been reported that very thin amorphous oxide films can form at the surfaces of liquid Ga and Al.[6,7] A monolayer of amorphous alumina was found in the initial oxidation of liquid Al at an oxygen partial pressure of 3×10^{-3} Torr.[6] With surface x-ray scattering techniques, an amorphous Ga oxide film with a well defined thickness of 0.5 nm was identified at room temperature on the oxygen partial pressure of 1.8×10^{-4} Torr, and didn't change with oxygen partial pressure up to 1.6×10^{-3} Torr nor at temperatures up to 300 ^{o}C.[7] It is anticipated that the formation of an amorphous Ga_2O_3 film is easier on a disordered substrate like a LM than a crystalline film.[7] However, little is understood of the thermodynamic stability of initial oxide growth on the LMs, which could be responsible for the scattered data of surface tensions in the literature.[2]

On the other hand, the development of initial oxide overgrowths on bare solid metal surfaces has been studied in detail, and it has been found that at relatively low temperatures often a thin (<10 nm) amorphous oxide film is formed on the surface of solid metals (e.g. Si, Ta, Nb, Al, Ge, Cr and Te), whereas at higher temperatures thicker films develop and the resulting structure of the corresponding oxide film is in most cases crystalline.[8-10] Mittemeijer and co-workers[11,12] developed a thermodynamic model, in which the energetics of the amorphous oxide film with thickness h_a on a bare single-crystalline metal substrate (M) can be compared with those of the corresponding crystalline oxide film with equivalent thickness h_a on M. This model has been applied to analyze the preferred formation of either an amorphous or a crystalline oxide overgrowth. On the basis of thermodynamic model calculations, they demonstrated that an amorphous oxide phase for the initial oxide overgrowth on a metal can be thermodynamically stable up to a certain critical thickness as long as the higher bulk energy of the amorphous oxide phase (as compared to that of the competing crystalline oxide phase) can be overcompensated for by the lower sum of the surface and interface energies for the amorphous oxide-film configuration. The thermodynamic model has been applied to the cases for a range of metal/oxide systems (oxidation of Al, Ni, Cu, Cr, Fe, Mg, Zr and Ti etc), and the predictions in the solid Al/Al_2O_3 system according to this model agree well with high resolution transmission electron microscopy (HRTEM) observations.[13]

In the present study, we follow closely the treatment of Mittemeijer and co-workers[11,12] to investigate the thermodynamic stability in the initial oxide growth of liquid Al, Mg and Ga. A thermodynamic model will be developed to obtain the critical thickness of thermodynamically stable amorphous oxide film through comparing the bulk, surface and interfacial energy differences between the amorphous and crystalline oxides. In contrast to the interface between oxide film and solid metal in the initial oxidation on a bare metal substrate, the interfacial energy between oxide film and liquid metals in this work was employed to compare the interfacial energy difference between the amorphous phase and the crystalline phase in the thermodynamic model calculations. The predictions, as obtained by application of the model to the liquid Al-Al_2O_3, liquid Mg/MgO and Ga-Ga_2O_3 systems, are compared with the experimental data available in the literature.

2. Theory and calculation

2.1 Basics of the model

Consider two situations for a homogeneous metal-oxide film M_xO_y of uniform thickness h on the surfaces of liquid metal (LM), as shown in Fig.1. The energetics of amorphous oxide film, $\{M_xO_y\}$, with thickness h_a on LM were compared with those of the corresponding crystalline oxide film, $<M_xO_y>$, with equivalent thickness h_c on LM. Cells of volumes $h_a \times l_a^2$ and $h_c \times l_c^2$ are defined for the amorphous oxide-film configuration and the corresponding crystalline one, respectively, with the same molar quantity of oxide. The difference in total Gibbs energy between the configurations at the growth temperature, T, can be given as:[11]

$$\Delta G^{t} = h_a \cdot \left(\frac{\Delta G_a^f - \Delta G_c^f}{V_a}\right) + \gamma_a^s + \gamma_a^i - \chi \cdot (\gamma_c^s + \gamma_c^i) \qquad (1)$$

where ΔG_a^f and ΔG_c^f are the Gibbs energies of formation of the amorphous and crystalline oxide phases, respectively; V_a is the molar volume of the amorphous oxide; γ_a^s and γ_c^s are the surface energies of the amorphous and crystalline oxides in contact with the ambient, respectively; γ_a^i is the interfacial energy of the interface between the LMs and the amorphous oxide overgrowth; γ_c^i is the interfacial energy of the interface between the liquid metals and the crystalline oxide overgrowth; The ratio χ corresponds to the surface area ratio of the unstrained amorphous cell and crystalline cell at the growth temperature.

ΔG_c^f of a crystalline oxide phase is always lower than ΔG_a^f of the corresponding amorphous oxide phase below the melting point of the oxide phase, T_m, and therefore bulk thermodynamics always tend to stabilize the crystalline oxide overgrowth. However, it is possible that the higher bulk Gibbs energies of the amorphous oxide phase can be overcompensated for by its lower sum

of surface and interface energies, thereby stabilizing the amorphous oxide overgrowth up to a certain critical thickness, h_a^c.

2.2 Bulk energy differences

The difference between the bulk Gibbs energies of formation of the amorphous and the crystalline oxide overgrowths on the surface of LM per unit area

$$\Delta G^b = h_a \cdot (\frac{\Delta G_a^f - \Delta G_c^f}{V_a}) \quad (2)$$

is always positive , thereby stabilizing the crystalline oxide cell with increasing oxide-film thickness, h_a.[11]

The values for bulk Gibbs energies of oxide formation, ΔG_a^f and ΔG_c^f, were taken from the NIST-JANAF Thermochemical Tables.[14] The molar volumes, V_a and V_c, of the amorphous and crystalline oxides at room temperature were taken from the literature,[15-17] and listed in Table 1. The temperature dependence of V_a for the amorphous oxide film is taken to be the same as that of the corresponding crystalline oxide, as obtained from the corresponding linear thermal expansion coefficients, α.[18,19]

2.3 Surface energy differences

The surface energy difference between the amorphous and the crystalline oxide overgrowths on the liquid metal per unit area is given by

$$\Delta\gamma^s = \gamma_a^s - \chi \cdot \gamma_c^s. \quad (3)$$

$\Delta\gamma^s$ is generally negative, and therefore contributes to the thermodynamic stability of the amorphous phase.[11]

An estimate of the surface energy of an amorphous oxide, γ_a^m, at its melting point, T_m, is obtained from the empirical relationship between γ_a^m and the molar volume, V_c^0, of the corresponding crystalline oxide at T_0=298 K: [12]

$$\gamma_a^m \cong 1.764 \cdot k_B \cdot T_m \cdot (\frac{V_c^0}{N_A \cdot x})^{-2/3} - 0.0372 \qquad (Jm^{-2}) \quad (4)$$

where x is the number of metal ions per M_xO_y unit "molecule"; k_B is the Boltzmann's constant; N_A is the Avogadro's constant. The temperature dependence of the surface energy of liquid oxides was taken from the literatures.[20] The corresponding temperature coefficient, $\frac{\partial\gamma_a^s}{\partial T}$, for the most liquid oxides is negative with an average value of $-0.07(\pm0.05)\times10^{-3} Jm^{-2}K^{-1}$.[12] In the case of amorphous MgO and Ga_2O_3, no data is available from the literature and $\frac{\partial\gamma_a^s}{\partial T}$ was taken as the

average value of -0.07×10^{-3}Jm^{-2}K^{-1}. The surface energy of crystalline oxide, γ_c^m, at T_m and its corresponding temperature dependence, $\frac{\partial\gamma_c^s}{\partial T}$, were taken from the literature.[21-25] χ was obtained according to the following equation:[11]

$$\chi = (\frac{V_c}{V_a})^{2/3}. \quad (5)$$

2.4 Interfacial energy differences

2.4.1 The crystalline oxide-liquid metal interface energy

The energy of the crystalline oxide-LM interface, γ_c^i, can be expressed as the result of three additive energy contributions: (i) the negative interaction contribution, γ_c^{chem}, resulting from the chemical bonding between crystalline oxide and LM across the interface; (ii) the positive entropy contribution, γ_c^{entr}, due to the ordering (i.e. the decrease in configuration entropy) of LM near the interface with the crystalline oxide; (iii) the positive enthalpy contribution, γ_c^{enth}, arising from the relative increase in enthalpy of the crystalline oxide at the interface due to the liquid-type of bonding with LM at the interface:[11]

$$\gamma_c^i = \gamma_c^{chem} + \gamma_c^{entr} + \gamma_c^{enth}$$
$$= \frac{1/3\Delta H^{\infty}_{O in\langle M\rangle}}{A(O) in \langle M_xO_y\rangle} - \frac{T\Delta S_M}{A(M) in LM} + \frac{1/3 H_c^{fs}}{A(M) in \langle M_xO_y\rangle} \quad (6)$$

where $\Delta H^{\infty}_{O in\langle M\rangle}$ is the mixing enthalpy of 1 mol oxygen atoms at infinite dilution in <*M*>:[12]

$$\Delta H^{\infty}_{O in\langle M\rangle} \cong 1.2\Delta H_c^f + 1\times10^5 \quad (Jmol^{-1}) \quad (7)$$

where ΔH_c^{fm} is the enthalpy of oxide formation per mol oxygen; ΔS_M is the entropy difference between crystalline and LM per mol M; H_c^{fs} is the molar enthalpy of fusion of <M_xO_y>. The fraction 1/3 is a geometric factor assuming the shape of the Wigner-Seitz cell of oxygen in the oxide to be intermediate between a cube and a sphere; *A*(*O*) and *A*(*M*) in <M_xO_y> is the molar interface areas of oxygen and metal in the crystalline oxide, respectively; *A*(*M*) in *LM* is the molar interface areas of metal atoms in LM.

ΔH_c^f, ΔS_M and H_c^{fs} were obtained from the literature.[14,26] *A*(*O*) and *A*(*M*) in <M_xO_y>, *A*(*M*) in *LM* were calculated from the lattice spacing at the interfaces, or taken from the literature.[24] The

molar interfacial area of M at the interface of LM is considered as the area occupied by 1 mol M atoms at the most dense-packed {111} plane of α-Al.

2.4.2 The amorphous oxide-liquid metal interface energy

The energy of the amorphous oxide-liquid metal interface, γ_a^i, is assumed to be that of liquid/liquid interface. The liquid/liquid interfacial energy usually is relatively small. For example, the interface energy of liquid/liquid in immiscible Al-Bi, Al-In and Al-Pb binary systems are 0.0567, 0.0255 and 0.1255 $Jmol^{-1}$, respectively.[27] Antonow[28] suggested that liquid-liquid interfacial energy between two liquids A and B can be calculated as the difference between their surface tensions of A and B. Here γ_a^i is approximated as the difference between γ_{LM}^s and γ_a^s, in which γ_{LM}^s is the surface tension of LMs. The values of γ_{LM}^s and its corresponding temperature dependence, $\frac{\partial \gamma_{LM}^s}{\partial T}$, are taken from the literature.[29]

3 Results

3.1 Al/Al_2O_3

For oxide overgrowths on liquid Al, the amorphous oxide overgrowth competes with crystalline γ-Al_2O_3. The γ-Al_2O_3 {111} crystallographic plane is the most dense-packed, corresponding to the γ-Al_2O_3 surface with the lowest energy. And then the terminated plane of γ-Al_2O_3 will be {111} plane in the process of γ-Al_2O_3 nucleation and growth. Fig.2 exhibits bulk (ΔG^b), interfacial ($\Delta\gamma^i$) and surface energy ($\Delta\gamma^s$) differences, as well as the corresponding total Gibbs energy difference (ΔG^t) of the amorphous oxide overgrowth and the corresponding crystalline oxide overgrowth on the surface of liquid Al at 700 ^oC. The bulk Gibbs energy difference between {Al_2O_3} and < γ-Al_2O_3> cells for h_a=1 nm is about 0.8 Jm^{-2}. The contribution from negative energy term is governed by the corresponding interfacial energy difference, which is relatively large, about 1.0 Jm^{-2}, compared with the considerably small surface energy difference of 0.02 Jm^{-2}. The critical thickness h_a^c is then determined by the point at ΔG^t=0. The energy balance leads to a h_a^c of about 1.3 nm at 700 ^oC.

Fig.3 shows the critical oxide film thickness up to which the {Al_2O_3} overgrowth is thermodynamically preferred. It can be seen that h_a^c increases slightly with the increase of T in the temperature range of T=660~1050 ^oC. h_a^c is about 1.28 nm at 660 ^oC, and 1.62 nm at 1050 ^oC, corresponding to about 6~8 mono-layers (MLs). The bulk Gibbs energy difference between {Al_2O_3} and <Al_2O_3> decreases with the increase of T while the increase in the sum of surface

and interfacial terms is less significant, and as a consequence the amorphous oxide is thermodynamically stabilized further with *T* in the considered temperature range.

3.2 Mg/MgO

The most dense-packing MgO{111} plane was chosen for the <MgO> overgrowth on liquid Mg, competed with the amorphous oxide overgrowth. Fig.4 shows bulk, interfacial and surface energy differences, as well as the corresponding total Gibbs energy difference of the amorphous oxide overgrowth and the corresponding crystalline oxide overgrowth on the surface of liquid Mg for h_a=1.0 nm at 700 ^oC. The Mg-O bond is the highest among all metal/oxide systems studied here, resulting in the high interfacial energy between <MgO>, {MgO} and liquid Mg, compared with those in Al/Al_2O_3 system. The bulk energy difference between <MgO> and {MgO} is about 4.4 Jm^{-2}, much higher than that between <Al_2O_3> and {Al_2O_3}. The large bulk energy difference leads to a small h_a^c in the Mg/MgO system.

Fig.5 shows the dependence of h_a^c on *T*. h_a^c decreases with increase of *T* in the temperature range of 650 to 1050 ^oC. h_a^c is about 0.15 nm at 650 ^oC, i.e. less than 1 ML, suggesting that the amorphous oxide phase is thermodynamically unstable above T_m.

3.3 Ga/Ga_2O_3

The β-Ga_2O_3 {100} crystallographic plane has the lowest energy,[24] and was chosen for the < β-Ga_2O_3 > overgrowth on the surface of liquid Ga, competed with {Ga_2O_3} overgrowth. Fig.6 shows bulk, interfacial and surface energy differences, as well as the corresponding total Gibbs energy difference of the amorphous oxide overgrowth and the corresponding crystalline oxide overgrowth on the surface of liquid Ga for h_a=1.0 nm at 29 ^oC. The contribution of negative energy term is also governed by the corresponding interfacial energy difference between γ_a^i and γ_c^i. Fig.7 shows the dependence of h_a^c on temperature. It can be seen that h_a^c is almost independent of *T* in the temperature range of 29-327 ^oC. h_a^c is about 0.35 nm, i.e. 2MLs, at 29 ^oC, indicating that the amorphous oxide phase is thermodynamically preferred in the considered temperature range.

4. Discussion

Only a few experimental observations on the initial oxide overgrowth at free surface of liquid metals have been reported,[6,7,30] due to the difficulty in experimental operation. It was reported

that a monolayer of amorphous Al_2O_3 film can be formed in the initial oxidation of liquid Al at oxygen partial pressure of 3×10^{-3} Torr.[6] The prediction, according to the thermodynamic model calculation in the liquid Al-Al_2O_3 system, revealed that the critical thickness of thermodynamically stable amorphous phase is 6-8 MLs in the temperature range of 650~1050 ^{o}C. Therefore, the formation of an amorphous oxide monolayer is thermodynamically preferred in the initial oxidation of liquid Al. For the liquid Ga-Ga_2O_3 system, the calculated critical thickness of an amorphous oxide film is about 0.35 nm in the temperature range of 27-327 ^{o}C. The experimental observation confirmed that an amorphous Ga_2O_3 film with a thickness of 0.5 nm formed in the temperature range from room temperature to 300^{o}C and on the oxygen partial pressure of 1.8×10^{-4}~1.6×10^{-3} Torr.[7] It should be noted that the accuracy of the parameters used in the model calculation can affect the reliability of the predicted results to a certain extent. Given the errors in both the thermodynamic model calculation and the experimental observation, the predictions agree well with the experimental results. By contrast, for the liquid Mg-MgO system the predicted critical thickness of an amorphous oxide film is less than 1 ML in the temperature range of 650~1050 ^{o}C, i.e. the amorphous oxide phase is thermodynamically unstable in the initial oxidation of liquid Mg. No experimental observation on the structure of oxide film in the initial oxidation of liquid Mg had been reported, partially due to the very high evaporation pressure of Mg. However, oxidation of liquid Mg usually produces a discontinuous oxide film on the surface.[5] In the initial oxidation on a bare solid Mg, the predicted critical oxide-film thickness, up to which the amorphous {MgO} overgrowth is thermodynamically preferred, is below 1 ML for all Mg substrate orientations,[11] as confirmed by the experimental observation.[31,32] It implied that the prediction of the initial oxide overgrowth at the free surface of liquid Mg seemed to be acceptable.

Both the experimental observations and model predictions are indicative of the formation of an amorphous oxide film in the initial oxidation on liquid Al and Ga. In the Al and Ga oxide systems, the bulk energy difference between the amorphous and crystalline oxides is relatively small, and then the negative energy contribution from surface and interfacial energy difference can compensate the positive energy contribution for the bulk term. The energy balance of negative surface and interfacial terms and positive bulk term produce a thermodynamically stable amorphous phase up to a few MLs near T_m. However, the bulk energy difference is quite large for the Mg oxide systems, compared to that of the Al and Ga oxide systems. As a consequence, the positive energy term can't be compensated by the sum of surface and interfacial energy terms in at least 1 ML of MgO oxide film, resulting in thermodynamic instability of the amorphous phase.

Different from the initial oxide overgrowth on a bare solid metal surface,[11,12] the strain energy and dislocation contributions between the crystalline oxide and metal substrate are absent in the

interfacial energy term between the crystalline oxide and LM for the initial oxidation of LMs. In the initial oxide overgrowth on a bare solid metal surface, the strain and dislocation energies are positive energy terms and contribute to the thermodynamic stability of amorphous oxide overgrowth. However, the calculated sum of strain and dislocation energy contributions is relatively small and does not exceed the value of 0.5 Jm^{-2} for all metal/oxide systems studied in the literature.[12] The decrease in the bulk Gibbs energy difference between the amorphous and crystalline oxide phases with increasing growth temperature is also preferred to the thermodynamic stability of amorphous phase in the initial oxidation for both at the free surface of LMs and on a bare solid metal surface. In both cases, the temperature dependence of h_a^c is governed by the decrease in the bulk Gibbs energy difference. It is noted that h_a^c in the initial oxidation of liquid Al exhibits the same positive temperature dependence as that in the initial oxide overgrowth on the solid Al surfaces.[11] The predicted h_a^c in the initial oxidation on liquid Al is about 1.3 nm at 700 ^oC, much larger than that in the initial oxidation on solid Al, about 0.6 nm at 298 ^oC. It is suggested that the amorphous oxide phase formed during the oxidation on the solid Al can be further stabilized with an increase of temperature beyond T_m. Therefore, the amorphous phase observed in the initial oxidation at the free surface of liquid Al in the literature[6] is indeed thermodynamically preferred.

5. Summary

Based on the thermodynamic model for the oxide overgrowth on the solid metal surface developed recently by Mittemeijer and co-workers, we have developed a thermodynamic model to analyze the thermodynamic stability of oxide overgrowth on liquid metals. In the Al/Al_2O_3 and Ga/Ga_2O_3 systems, the thermodynamic model predictions revealed that the positive bulk Gibbs energy difference between amorphous and crystalline oxides can be compensated for up to a critical thickness of a few atomic layers by the negative energy difference of surface and interfacial terms, and thermodynamically stabilizes the amorphous oxide phase. However, the bulk Gibbs energy difference is relatively large for the Mg/MgO system, and can't be compensated for by the surface and interfacial energy difference. The critical thickness of thermodynamically preferred amorphous phase is about 1.3 nm for the $Al/\gamma\text{-}Al_2O_3$ and 0.33 nm for the $Ga/\ \beta\text{-}Ga_2O_3$ system, respectively, at the melting point of the LMs. The amorphous oxide is thermodynamically unstable for the Mg/MgO system.

Reference:

1. M. Merkwitz and W. Hoyer: *Z. Metallkd.*, 1999, 90, 363-370.
2. B. M. Gallois: *JOM Journal of the Minerals, Metals and Materials Society*, 1997, 49, 48-51.

3. H. Fujii, S. Izutani, T. Matsumoto, S. Kiguchi and K. Nogi: *Mater. Sci. Engi.* A, 2006, 417, 99-103.
4. S. A. Impey, D. J. Stephenson and J. R. Nicholls: *Mater. Sci. Technol.*, 1988, 4, 1126-1132.
5. S. P. Cashion, N. J. Ricketts and P. C. Hayes: J. Light Metals, 2002, 2, 43-47.
6. F. Stucki, M. Erbudak and G. Kostorz: *Appl. Surf. Sci.*, 1987, 27, 393-400.
7. M. J. Regan, H. Tostmann, P.S. Pershan, O. M. Magnussen, E. DiMasi, B. M. Ocko and M. Deutsch: *Phys. Rev.* B, 1997, 55, 10786-10790.
8. K. R. Lawless: *Rep. Prog. Phys.*, 1974, 37, 231-316.
9. L. P. H. Jeurgens, W. G. Sloof, F. D. Tichelaar and E. J. Mittemeijer: *J. Appl. Phys., 2002*, 92, 1649-1656.
10. L. P. H. Jeurgens, A. Lyapin and E. J. Mittemeijer: *Acta. Mater.*, 2005, 53, 4871-4879.
11. L.P.H.Jeurgens, W. G. Sloof, F. D. Tichelaar and E. J. Mittemeijer: *Phys. Rev*. B, 2000, 62, 4707-4719.
12. F. Reichel, L. P. H. Jeurgens and E. J. Mittemeijer: *Acta. Mater*., 2008, 56, 659-674.
13. K. Shinohara, T. Seo and H. Kyogoku: *Z. Metallkd*., 1982, 73, 774-780.
14. M. W. Chase Jr.: in 'NIST-JANAF thermochemical tables', 4th edn, 59-1539; 1998, J. Phys. Chem., Ref. Data.
15. W. J. Bernard and J. W. Cook: *J. Electrochem. Soc*., 1959, 106, 643-646.
16. A. Leu, S. Ma, and H. Eyring: *Proc. Nat. Acad. Sci. USA*, 1975, 72, 1026-1030.
17. D. B. Dingwell: *J. Am. Ceram. Soc*., 1992, 75, 1656-1657.
18. Y. S. Touloukian, R. K. Kirby, R. E. Taylor and T. Y. R. Lee: 'Thermal expansion: Nonmetallic solids, Thermophysical properties of matter', Vol.13, 2-200; 1977, New York, IFI/Plenum.
19. H. Yanagida and G. Yamaguchi: *Bull. Chem. Soc. Jpn*., 1964, 37, 1229-1231.
20. N. Ikemiya, J. Umemoto, S. Hara and K.Ogino: *ISIJ Int.*, 1993, 33, 156-165.
21. S. Blonski and S. H. Garofalini: *Surf. Sci.*, 1993, 295, 263-274.
22. J. J. Gilman: *J. Appl. Phys*., 1960, 31, 2208-2218.
23. G. Jura and C. W. Garland: *J. Am. Chem. Soc*., 1952, 74, 6033-6034.
24. V. M. Bermudez: *Chem. Phys.*, 2006, 323, 193-203.
25. N. Zouvelou, D. Skarmoutsos and P. Nikolopoulos: *Key Eng. Mater.*, 2004, 679, 264-268.
26. R. C. Weast: 'Handbook of chemistry and physics', 55th edn, 22-31; 1974, CRC, Ohio.
27. W. Hoyer, I. Kaban and M. Merkwitz: *J. Opt. Adv. Mater.*, 2003, 5, 1069-1073.
28. G.N. Antonow: *J. Chem. Phys*., 1907, 5, 372-384.
29. T. Iida and R. I. L. Guthrie: 'The physical properties of liquid metals', 133-134; 1988, Oxford, Clarendon.
30. A.J. Bevolo, J. D. Verhoeven and M. Noack: *Surf. Sci.*, 1983, 134, 499-528.
31. L.P.H. Jeurgens, M.S. Vinodh and E. J. Mittemeijer: *Acta. Mater*., 2008, 56, 4621-4634.
32. M. Kurth, P. C. J. Graat, H. D. Carstanjen and E. J. Mittemeijer: *Surf. Interface Anal.*, 2006, 38, 931-940.

Table 1 Physical data of the Al/Al_2O_3, Mg/MgO and Ga/Ga_2O_3 (T_0=298°C).

Surface	Symbol	Value	Unit	Ref.
		molar volumes at T_0		
$\{Al_2O_3\}$	V_a^o	3.19×10^{-5}	m^3mole^{-1}	15
$<\gamma\text{-}Al_2O_3>$	V_c^o	2.81×10^{-5}	m^3mole^{-1}	15
{MgO}	V_a^o	5.42×10^{-5}	m^3mole^{-1}	16
<MgO>	V_c^o	1.10×10^{-5}	m^3mole^{-1}	16
$\{Ga_2O_3\}$	V_a^o	3.81×10^{-5}	m^3mole^{-1}	17
$<\beta\text{-}Ga_2O_3>$	V_c^o	3.19×10^{-5}	m^3mole^{-1}	17
		coefficients of linear thermal expansion $\alpha(T)=a+b\cdot\Delta T$		
$<\gamma\text{-}Al_2O_3>$	a	$=2.068\times10^{-6}$	K^{-1}	19
	b	$=1.1499\times10^{-8}$	K^{-2}	19
<MgO>	a	$=11.0\times10^{-6}$	K^{-1}	16
	b	$=6.0\times10^{-10}$	K^{-2}	16
$<\beta\text{-}Ga_2O_3>$	a	$=-2.0\times10^{-6}$	K^{-1}	27
	b	=0	K^{-2}	27
		surface energies at T_m		
$<\gamma\text{-}Al_2O_3>\{111\}$	γ_c^m	0.94	Jm^{-2}	21
<MgO>	γ_c^m	2.53	Jm^{-2}	22,23
$<\beta\text{-}Ga_2O_3>\{100\}$	γ_c^m	1.13	Jm^{-2}	24
liquid Al	γ_{LM}^m	0.914	Jm^{-2}	29
liquid Mg	γ_{LM}^m	0.559	Jm^{-2}	29
liquid Ga	γ_{LM}^m	0.718	Jm^{-2}	29
		temperature coefficient of surface energies		
$\{Al_2O_3\}$	$\partial\gamma_a^s/\partial T$	-0.187×10^{-3}	$Jm^{-2}k^{-1}$	20
$<\gamma\text{-}Al_2O_3>$	$\partial\gamma_c^s/\partial T$	-0.5×10^{-3}	$Jm^{-2}k^{-1}$	12
{MgO}	$\partial\gamma_a^s/\partial T$	0.07×10^{-3}	$Jm^{-2}k^{-1}$	12
<MgO>	$\partial\gamma_c^s/\partial T$	-0.476×10^{-3}	$Jm^{-2}k^{-1}$	25
$\{Ga_2O_3\}$	$\partial\gamma_a^s/\partial T$	$+0.04\times10^{-3}$	$Jm^{-2}k^{-1}$	12
$<\beta\text{-}Ga_2O_3>$	$\partial\gamma_c^s/\partial T$	-0.4×10^{-3}	$Jm^{-2}k^{-1}$	12
liquid Al	$\partial\gamma_{LM}^s/\partial T$	-0.35×10^{-3}	$Jm^{-2}k^{-1}$	29
liquid Mg	$\partial\gamma_{LM}^s/\partial T$	-0.35×10^{-3}	$Jm^{-2}k^{-1}$	29
liquid Ga	$\partial\gamma_{LM}^s/\partial T$	-0.10×10^{-3}	$Jm^{-2}k^{-1}$	29

Figure captions:

Fig.1 Schematic drawing of a homogeneous M_xO_y oxide film with uniform thickness on the surface of liquid metals (*LM*s). (a) An amorphous oxide film $\{M_xO_y\}$ with thickness of h_a; (b) A crystalline oxide $<M_xO_y>$ film with a thickness of h_c (the braces {} refer to the amorphous phase, and the brackets <> to the crystalline phase). Amorphous cell $h_a \times l_a^2$ in (a) and crystalline cell $h_c \times l_c^2$ in (b) have the same composition, formed from the same molar quantity of oxygen on the surface of an identical *LM*.

Fig.2 Bulk (ΔG^b), interfacial ($\Delta\gamma^i$) and surface energy ($\Delta\gamma^s$) differences, as well as the corresponding total Gibbs energy difference ($\Delta G^t=\Delta G^b+\Delta\gamma^s+\Delta\gamma^i$), as functions of oxide-film thickness (h_a) for the amorphous oxide $\{Al_2O_3\}$ overgrowth and the corresponding crystalline $<\gamma\text{-}Al_2O_3>$ oxide overgrowth on the surface of liquid Al at a growth temperature of 700 ^oC. The positive ΔG^b increases with h_a, however the sum of negative $\Delta\gamma^s$ and $\Delta\gamma^i$ terms is independent of h_a. The critical thickness h_a^c is determined by the point at $\Delta G^t=0$. h_a^c is about 1.3 nm at 700 ^oC (as indicated by the arrow).

Fig.3 Temperature dependence of critical thickness h_a^c for the amorphous $\{Al_2O_3\}$ oxide overgrowth in the initial oxidation on liquid Al. On the surface of liquid Al, the amorphous oxide overgrowth was competed with the crystalline $<\gamma\text{-}Al_2O_3>$ oxide overgrowth with {111} crystallographic plane as the terminated surface. h_a^c is 1.28 nm at 660 ^oC, and increases slightly with T. Below h_a^c, an amorphous oxide film is thermodynamically preferred than a crystalline film.

Fig.4 ΔG^b, $\Delta\gamma^i$, $\Delta\gamma^s$ and ΔG^t as functions of h_a for the amorphous oxide $\{MgO\}$ overgrowth and the corresponding crystalline $<MgO>$ oxide overgrowth on the surface of liquid Mg at a growth temperature of 700 ^oC. The positive ΔG^b term increases rapidly with h_a, and leads to the thermodynamic instability of the amorphous phase. The relatively large ΔG^b suppresses the critical thickness up to h_a^c=0.15 nm.

Fig.5 Temperature dependence of h_a^c for the amorphous $\{MgO\}$ oxide overgrowth in the initial oxidation on liquid Mg. h_a^c is 0.15 nm at 650 ^oC, and decreases further with T. h_a^c is less than 1ML at 650 ^oC, suggesting that an amorphous oxide film is thermodynamically unstable in the considered temperature range. A crystalline <MgO> oxide film instead of an amorphous oxide film is thermodynamically preferred on the surface of liquid Mg.

Fig.6 ΔG^b, $\Delta\gamma^i$, $\Delta\gamma^s$ and ΔG^t as functions of h_a for the amorphous oxide $\{Ga_2O_3\}$ overgrowth and the corresponding crystalline $<\beta\text{-}Ga_2O_3>$ oxide overgrowth on the surface of liquid Ga at a growth temperature of 29 ^oC. The positive ΔG^b term can be compensated up to h_a^c of 0.35 nm at 29 ^oC (as indicated by the arrow) by the sum of negative $\Delta\gamma^s$ and $\Delta\gamma^i$ terms.

Fig.7 Temperature dependence of h_a^c for the amorphous $\{Ga_2O_3\}$ oxide overgrowth in the initial oxidation on liquid Ga. On the surface of liquid Ga, the amorphous oxide overgrowth was competed with the crystalline $<\beta\text{-}Ga_2O_3>$ oxide overgrowth. The calculated h_a^c is nearly independent of T in the considered temperature range. h_a^c=0.35 nm (about 2 MLs) at 29 ^oC, indicating that an amorphous $\{Ga_2O_3\}$ oxide overgrowth instead of a crystalline oxide overgrowth is thermodynamically preferred.

Figures:

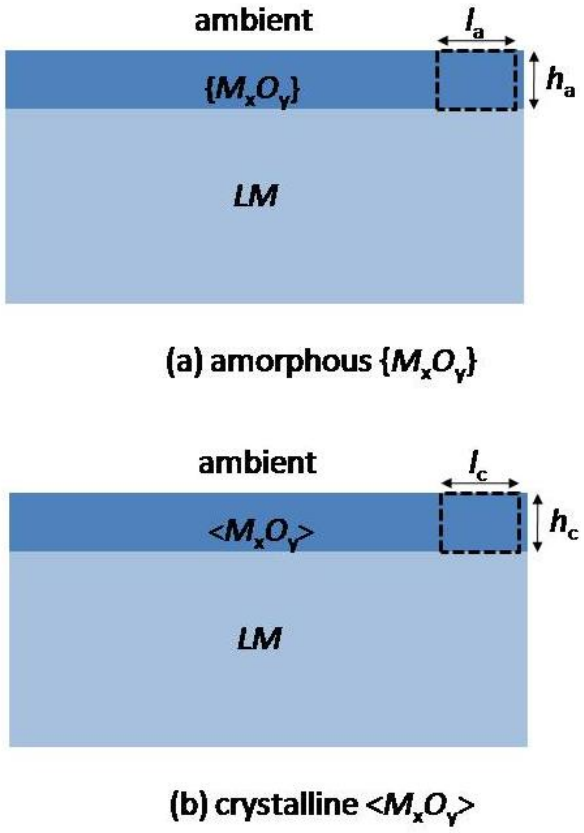

Fig.1

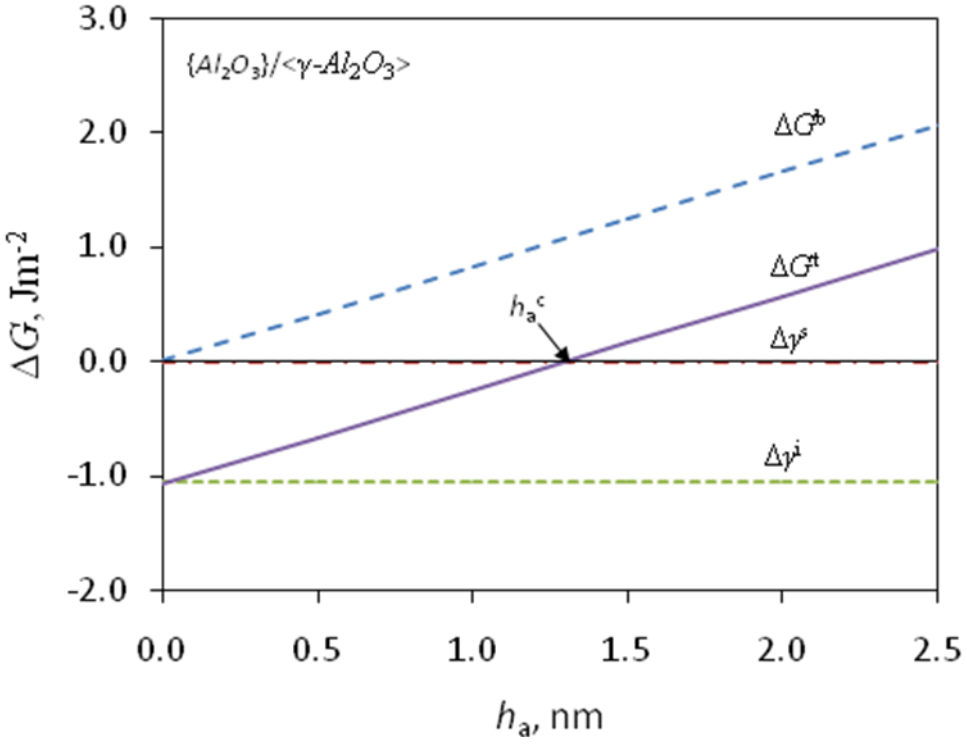
{Al2O3}/<γ-Al2O3>
ΔG^b
ΔG^t
h_a^c
Δγ^s
Δγ^i
ΔG, Jm-2
h_a, nm
3.0
2.0
1.0
0.0
-1.0
-2.0
0.0
0.5
1.0
1.5
2.0
2.5

Fig.2

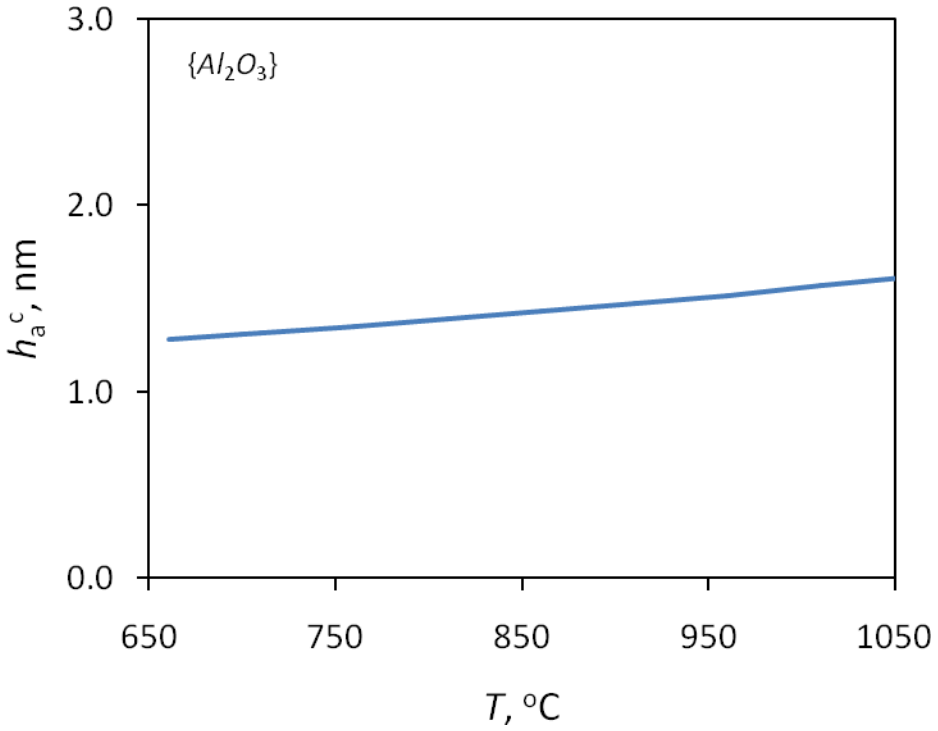

Fig.3

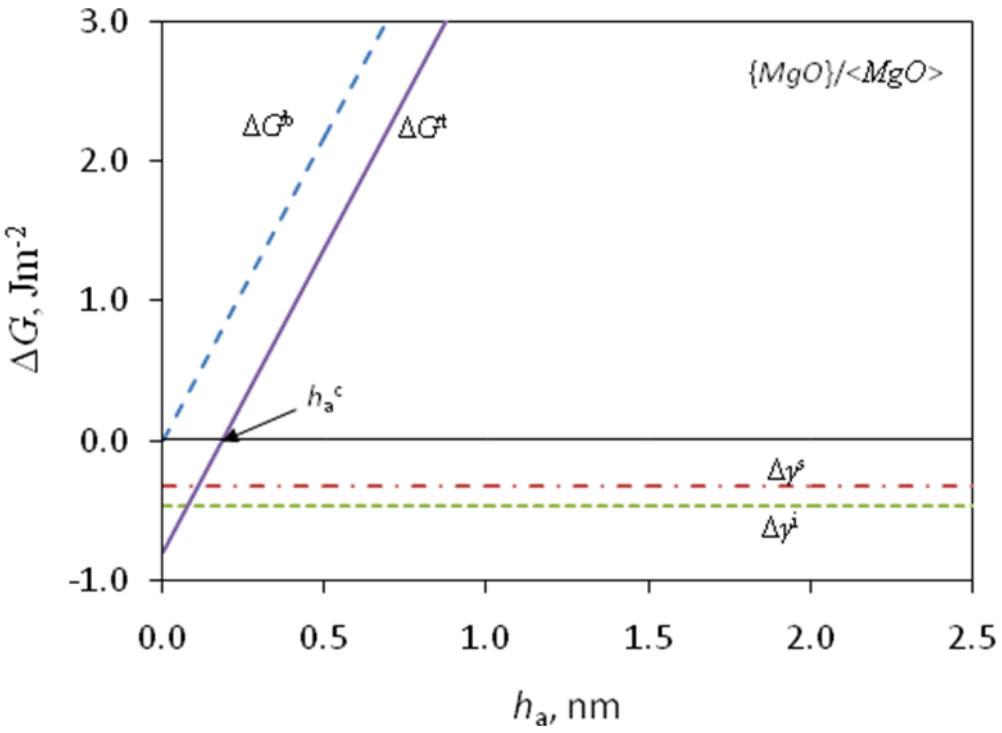
3.0
2.0
1.0
0.0
-1.0
0.0
0.5
1.0
1.5
2.0
2.5
ΔG, Jm-2
ha, nm
{MgO}/<MgO>
ΔGb
ΔGt
ha c
Δγs
Δγi

Fig.4

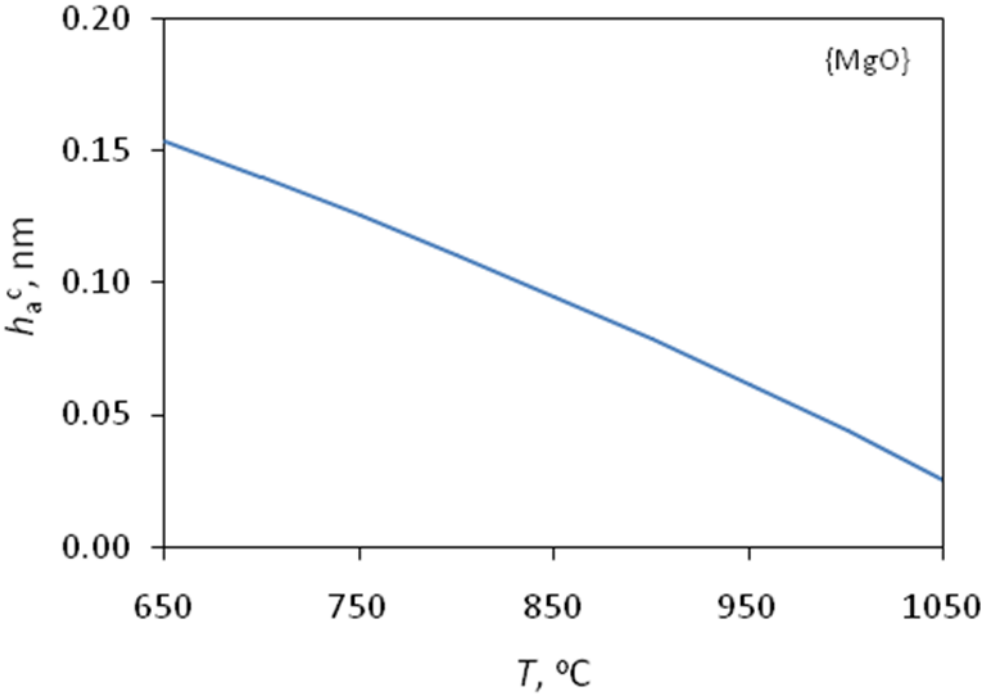

Fig.5

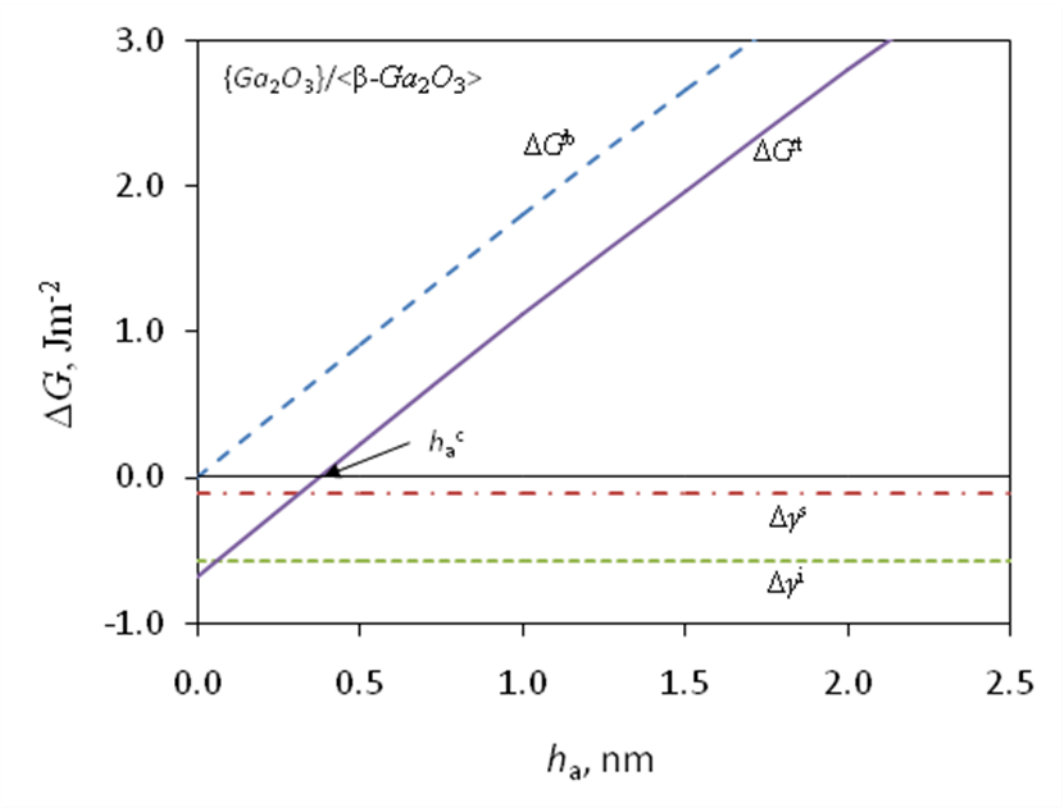
{Ga2O3}/<β-Ga2O3>
ΔGb
ΔGt
ha c
Δγs
Δγi
ΔG, Jm-2
ha, nm
3.0
2.0
1.0
0.0
-1.0
0.0
0.5
1.0
1.5
2.0
2.5

Fig. 6

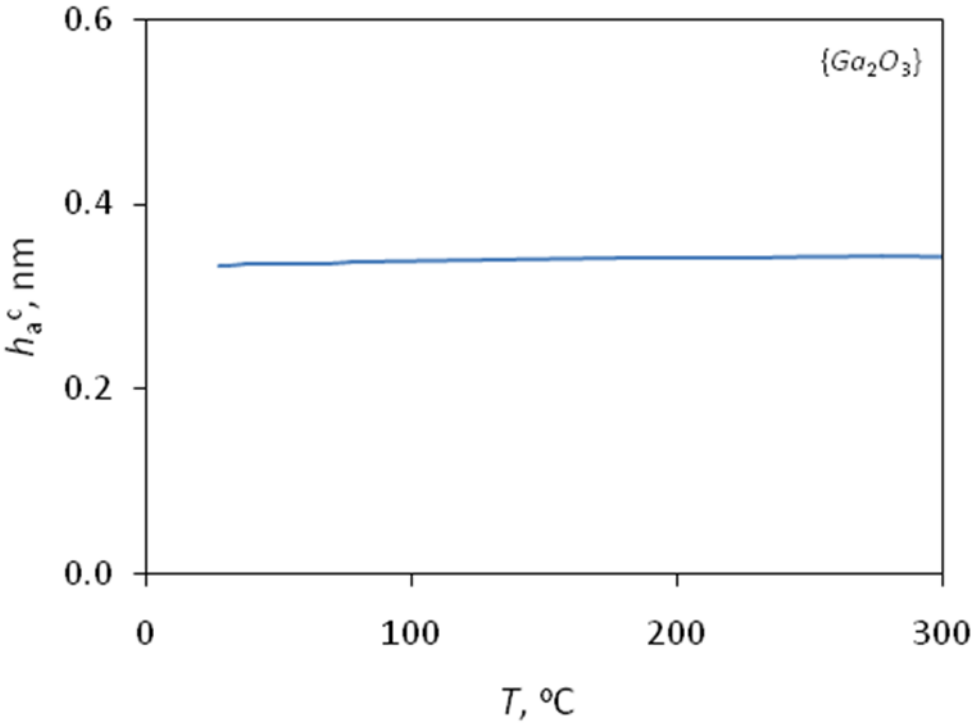

Fig.7

Response to the comments

We revised the manuscript "Transition of amorphous to crystalline oxide film in initial oxide overgrowth on liquid metals" (Ref: MST9464), according the comments of reviewer.

The changes are:

(1) "For example, an atomic scale oxide-free aluminum surface in thermodynamic equilibrium is not easy to achieve because the maximum oxygen partial pressure that is in equilibrium with physically dissolved oxygen is very low (up to 10^{-4}bar)."

We adopted the new value "10^{-4}bar" from the recent literatures, instead of "10^{-40}bar" from the traditional literature.

(2) Correspondingly, the following literatures were included in the manuscript:

[2]D. Giuranno, E. Ricci, E. Arato and P. Costa: *Acta Mater*., 2006,54,2625-2630.
[3]J. M. Molina, R. Voytovych, E. Louis and N. Eustathopoulos: *Int. J. Adhes. Adhes*., 2007, 27, 394-401.

Transition of amorphous to crystalline oxide film in initial oxide overgrowth on liquid metals

H. Men[1,2], Z. Fan[1,2*]

[1]LiME (EPSRC Centre for Innovative Manufacturing in Liquid Metal Engineering),

[2]BCAST (Brunel Centre for Advanced Solidification Technology),

Brunel University, Uxbridge, Middlesex, UB8 3PH, UK

Abstract

It is important to understand the mechanism of oxidation in the initial stage at free surface on liquid metals. Mittemeijer and co-workers recently developed a thermodynamic model to study the oxide overgrowth on a solid metal surface. Based on this model, we have developed a thermodynamic model to analyze the thermodynamic stability of oxide overgrowth on liquid metals. The thermodynamic model calculation revealed that the amorphous oxide phase is thermodynamically preferred up to 1.3 and 0.35nm, respectively, in the initial oxide overgrowth on liquid Al and Ga at the corresponding melting point. However, the amorphous phase is thermodynamically unstable in the initial oxide overgrowth on liquid Mg. The thermodynamic stability of amorphous phase in the Al and Ga oxide systems is attributed to lower sums of surface and interfacial energies for amorphous phases, compared to that of the corresponding crystalline phases.

Keywords: Thermodynamics; Oxidation; Liquid metal; Amorphous phase

1. Introduction

Research on oxidation at free surfaces of liquid metals (LMs) is of the fundamental and scientific interests. Oxide films easily form on the free surface of LMs even under high vacuum conditions, especially for reactive elements such as Al and Mg. For example, an atomic scale oxide-free aluminum surface in thermodynamic equilibrium is not easy to achieve because the maximum oxygen partial pressure that is in equilibrium with physically dissolved oxygen is very low (up to

* Corresponding author. Tel.: +44 1895 266406; fax: +44 1895 269758.
E-mail address: Zhongyun.Fan@brunel.ac.uk (Z. Fan).

10^{-4}bar).[1-3] Surface oxidation of LMs can dramatically change the surface tension which will have a significant effect on the way LMs wet different surfaces.[4,5] This is important for the process, such as soldering, brazing, casting and so on. There are considerable differences between the ways oxidation develops in various LMs. For example, the formation of a relatively thin surface oxide layer (e.g. an Al_2O_3 oxide film at the surface of liquid Al) effectively prevents the bulk from further oxidation to reduce melt losses (2~10% for Al alloys) during melting.[6] On the other hand, oxidation of liquid Mg produces a discontinuous oxide film.[7]

It has been reported that very thin amorphous oxide films can form at the surfaces of liquid Ga and Al.[8,9] A monolayer of amorphous alumina was found in the initial oxidation of liquid Al at an oxygen partial pressure of 3×10^{-3}Torr.[8] With surface x-ray scattering techniques, an amorphous Ga oxide film with a well defined thickness of 0.5nm was identified at room temperature on the oxygen partial pressure of 1.8×10^{-4}Torr, and didn't change with oxygen partial pressure up to 1.6×10^{-3}Torr nor at temperatures up to 300^{o}C.[9] It is anticipated that the formation of an amorphous Ga_2O_3 film is easier on a disordered substrate like a LM than a crystalline film.[9] However, little is understood of the thermodynamic stability of initial oxide growth on the LMs, which could be responsible for the scattered data of surface tensions in the literature.[4]

On the other hand, the development of initial oxide overgrowths on bare solid metal surfaces has been studied in detail, and it has been found that at relatively low temperatures often a thin (<10nm) amorphous oxide film is formed on the surface of solid metals (e.g. Si, Ta, Nb, Al, Ge, Cr and Te), whereas at higher temperatures thicker films develop and the resulting structure of the corresponding oxide film is in most cases crystalline.[10-12] Mittemeijer and co-workers[13,14] developed a thermodynamic model, in which the energetics of the amorphous oxide film with thickness h_a on a bare single-crystalline metal substrate (M) can be compared with those of the corresponding crystalline oxide film with equivalent thickness h_a on M. This model has been applied to analyse the preferred formation of either an amorphous or a crystalline oxide overgrowth. On the basis of thermodynamic model calculations, they demonstrated that an amorphous oxide phase for the initial oxide overgrowth on a metal can be thermodynamically stable up to a certain critical thickness as long as the higher bulk energy of the amorphous oxide phase (as compared to that of the competing crystalline oxide phase) can be overcompensated for by the lower sum of the surface and interface energies for the amorphous oxide-film configuration. The thermodynamic model has been applied to the cases for a range of metal/oxide systems (oxidation of Al, Ni, Cu, Cr, Fe, Mg, Zr and Ti etc), and the predictions in the solid Al/Al_2O_3 system according to this model agree well with high resolution transmission electron microscopy (HRTEM) observations.[15]

In the present study, we follow closely the treatment of Mittemeijer and co-workers[13,14] to investigate the thermodynamic stability in the initial oxide growth of liquid Al, Mg and Ga. A thermodynamic model will be developed to obtain the critical thickness of thermodynamically stable amorphous oxide film through comparing the bulk, surface and interfacial energy differences between the amorphous and crystalline oxides. In contrast to the interface between oxide film and solid metal in the initial oxidation on a bare metal substrate, the interfacial energy between oxide film and liquid metals in this work was employed to compare the interfacial energy difference between the amorphous phase and the crystalline phase in the thermodynamic model calculations. The predictions, as obtained by application of the model to the liquid Al-Al_2O_3, liquid Mg/MgO and Ga-Ga_2O_3 systems, are compared with the experimental data available in the literature.

2. Theory and calculation

2.1 Basics of the model

Consider two situations for a homogeneous metal-oxide film M_xO_y of uniform thickness h on the surfaces of liquid metal (LM), as shown in Fig. 1. The energetics of amorphous oxide film, $\{M_xO_y\}$, with thickness h_a on LM were compared with those of the corresponding crystalline oxide film, $<M_xO_y>$, with equivalent thickness h_c on LM. Cells of volumes $h_a \times l_a^2$ and $h_c \times l_c^2$ are defined for the amorphous oxide-film configuration and the corresponding crystalline one, respectively, with the same molar quantity of oxide. The difference in total Gibbs energy between the configurations at the growth temperature, T, can be given as:[13]

$$\Delta G^{t} = h_a \cdot \left(\frac{\Delta G_a^f - \Delta G_c^f}{V_a}\right) + \gamma_a^s + \gamma_a^i - \chi \cdot (\gamma_c^s + \gamma_c^i) \quad (1)$$

where ΔG_a^f and ΔG_c^f are the Gibbs energies of formation of the amorphous and crystalline oxide phases, respectively; V_a is the molar volume of the amorphous oxide; γ_a^s and γ_c^s are the surface energies of the amorphous and crystalline oxides in contact with the ambient, respectively; γ_a^i is the interfacial energy of the interface between the LMs and the amorphous oxide overgrowth; γ_c^i is the interfacial energy of the interface between the liquid metals and the crystalline oxide overgrowth; The ratio χ corresponds to the surface area ratio of the unstrained amorphous cell and crystalline cell at the growth temperature.

ΔG_c^f of a crystalline oxide phase is always lower than ΔG_a^f of the corresponding amorphous oxide phase below the melting point of the oxide phase, T_m, and therefore bulk thermodynamics always tend to stabilize the crystalline oxide overgrowth. However, it is possible that the higher

bulk Gibbs energies of the amorphous oxide phase can be overcompensated for by its lower sum of surface and interface energies, thereby stabilizing the amorphous oxide overgrowth up to a certain critical thickness, h_a^c.

2.2 Bulk energy differences

The difference between the bulk Gibbs energies of formation of the amorphous and the crystalline oxide overgrowths on the surface of LM per unit area

$$\Delta G^b = h_a \cdot (\frac{\Delta G_a^f - \Delta G_c^f}{V_a}) \qquad (2)$$

is always positive , thereby stabilizing the crystalline oxide cell with increasing oxide-film thickness, h_a.[13]

The values for bulk Gibbs energies of oxide formation, ΔG_a^f and ΔG_c^f, were taken from the NIST-JANAF Thermochemical Tables.[16] The molar volumes, V_a and V_c, of the amorphous and crystalline oxides at room temperature were taken from the literature,[17-19] and listed in Table 1. The temperature dependence of V_a for the amorphous oxide film is taken to be the same as that of the corresponding crystalline oxide, as obtained from the corresponding linear thermal expansion coefficients, α.[20,21]

2.3 Surface energy differences

The surface energy difference between the amorphous and the crystalline oxide overgrowths on the liquid metal per unit area is given by

$$\Delta\gamma^s = \gamma_a^s - \chi \cdot \gamma_c^s . \qquad (3)$$

$\Delta\gamma^s$ is generally negative, and therefore contributes to the thermodynamic stability of the amorphous phase.[13]

An estimate of the surface energy of an amorphous oxide, γ_a^m, at its melting point, T_m, is obtained from the empirical relationship between γ_a^m and the molar volume, V_c^0, of the corresponding crystalline oxide at T_0=298K: [14]

$$\gamma_a^m \cong 1.764 \cdot k_B \cdot T_m \cdot (\frac{V_c^0}{N_A \cdot x})^{-2/3} - 0.0372 \qquad (Jm^{-2}) \qquad (4)$$

where x is the number of metal ions per M_xO_y unit "molecule"; k_B is the Boltzmann's constant; N_A is the Avogadro's constant. The temperature dependence of the surface energy of liquid oxides was taken from the literatures.[22] The corresponding temperature coefficient, $\frac{\partial\gamma_a^s}{\partial T}$, for the most liquid oxides is negative with an average value of $-0.07(\pm0.05)\times10^{-3}Jm^{-2}K^{-1}$.[14] In the case

of amorphous MgO and Ga_2O_3, no data is available from the literature and $\frac{\partial \gamma_a^s}{\partial T}$ was taken as the average value of -0.07×10^{-3}Jm^{-2}K^{-1}. The surface energy of crystalline oxide, γ_c^m, at T_m and its corresponding temperature dependence, $\frac{\partial \gamma_c^s}{\partial T}$, were taken from the literature.[23-27] χ was obtained according to the following equation:[13]

$$\chi = (\frac{V_c}{V_a})^{2/3}. \quad (5)$$

2.4 Interfacial energy differences

2.4.1 The crystalline oxide-liquid metal interface energy

The energy of the crystalline oxide-LM interface, γ_c^i, can be expressed as the result of three additive energy contributions: (i) the negative interaction contribution, γ_c^{chem}, resulting from the chemical bonding between crystalline oxide and LM across the interface; (ii) the positive entropy contribution, γ_c^{entr}, due to the ordering (i.e. the decrease in configuration entropy) of LM near the interface with the crystalline oxide; (iii) the positive enthalpy contribution, γ_c^{enth}, arising from the relative increase in enthalpy of the crystalline oxide at the interface due to the liquid-type of bonding with LM at the interface:[13]

$$\gamma_c^i = \gamma_c^{chem} + \gamma_c^{entr} + \gamma_c^{enth}$$
$$= \frac{1/3\Delta H^{\infty}_{O in\langle M\rangle}}{A(O) in \langle M_xO_y\rangle} - \frac{T\Delta S_M}{A(M) in LM} + \frac{1/3 H_c^{fs}}{A(M) in \langle M_xO_y\rangle} \quad (6)$$

where $\Delta H^{\infty}_{O in\langle M\rangle}$ is the mixing enthalpy of 1mol oxygen atoms at infinite dilution in <*M*>:[14]

$$\Delta H^{\infty}_{O in\langle M\rangle} \cong 1.2\Delta H_c^f + 1\times10^5 \quad (Jmol^{-1}) \quad (7)$$

where ΔH_c^{fm} is the enthalpy of oxide formation per mol oxygen; ΔS_M is the entropy difference between crystalline and LM per mol M; H_c^{fs} is the molar enthalpy of fusion of <M_xO_y>. The fraction 1/3 is a geometric factor assuming the shape of the Wigner-Seitz cell of oxygen in the oxide to be intermediate between a cube and a sphere; *A*(*O*) and *A*(*M*) in <M_xO_y> is the molar interface areas of oxygen and metal in the crystalline oxide, respectively; *A*(*M*) in *LM* is the molar interface areas of metal atoms in LM.

ΔH_c^f, ΔS_M and H_c^{fs} were obtained from the literature.[16,28] $A(O)$ and $A(M)$ in $<M_xO_y>$, $A(M)$ in LM were calculated from the lattice spacing at the interfaces, or taken from the literature.[26] The molar interfacial area of M at the interface of LM is considered as the area occupied by 1mol M atoms at the most dense-packed {111} plane of α-Al.

2.4.2 The amorphous oxide-liquid metal interface energy

The energy of the amorphous oxide-liquid metal interface, γ_a^i, is assumed to be that of liquid/liquid interface. The liquid/liquid interfacial energy usually is relatively small. For example, the interface energy of liquid/liquid in immiscible Al-Bi, Al-In and Al-Pb binary systems are 0.0567, 0.0255 and 0.1255Jmol^{-1}, respectively.[29] Antonow[30] suggested that liquid-liquid interfacial energy between two liquids A and B can be calculated as the difference between their surface tensions of A and B. Here γ_a^i is approximated as the difference between γ_{LM}^s and γ_a^s, in which γ_{LM}^s is the surface tension of LMs. The values of γ_{LM}^s and its corresponding temperature dependence, $\frac{\partial \gamma_{LM}^s}{\partial T}$, are taken from the literature.[31]

3 Results

3.1 Al/Al_2O_3

For oxide overgrowths on liquid Al, the amorphous oxide overgrowth competes with crystalline γ-Al_2O_3. The γ-Al_2O_3 {111} crystallographic plane is the most dense-packed, corresponding to the γ-Al_2O_3 surface with the lowest energy. And then the terminated plane of γ-Al_2O_3 will be {111} plane in the process of γ-Al_2O_3 nucleation and growth. Fig. 2 exhibits bulk (ΔG^b), interfacial ($\Delta\gamma^i$) and surface energy ($\Delta\gamma^s$) differences, as well as the corresponding total Gibbs energy difference (ΔG^t) of the amorphous oxide overgrowth and the corresponding crystalline oxide overgrowth on the surface of liquid Al at 700^{o}C. The bulk Gibbs energy difference between {Al_2O_3} and < γ-Al_2O_3> cells for h_a=1nm is about 0.8Jm^{-2}. The contribution from negative energy term is governed by the corresponding interfacial energy difference, which is relatively large, about 1.0Jm^{-2}, compared with the considerably small surface energy difference of 0.02Jm^{-2}. The critical thickness h_a^c is then determined by the point at ΔG^t=0. The energy balance leads to a h_a^c of about 1.3nm at 700^{o}C.

Fig. 3 shows the critical oxide film thickness up to which the {Al_2O_3} overgrowth is thermodynamically preferred. It can be seen that h_a^c increases slightly with the increase of T in

the temperature range of T=660~1050^{o}C. h_a^c is about 1.28nm at 660^{o}C, and 1.62nm at 1050^{o}C, corresponding to about 6~8 mono-layers (MLs). The bulk Gibbs energy difference between {Al_2O_3} and <Al_2O_3> decreases with the increase of T while the increase in the sum of surface and interfacial terms is less significant, and as a consequence the amorphous oxide is thermodynamically stabilized further with T in the considered temperature range.

3.2 Mg/MgO

The most dense-packing MgO{111} plane was chosen for the <MgO> overgrowth on liquid Mg, competed with the amorphous oxide overgrowth. Fig. 4 shows bulk, interfacial and surface energy differences, as well as the corresponding total Gibbs energy difference of the amorphous oxide overgrowth and the corresponding crystalline oxide overgrowth on the surface of liquid Mg for h_a=1.0nm at 700^{o}C. The Mg-O bond is the highest among all metal/oxide systems studied here, resulting in the high interfacial energy between <MgO>, {MgO} and liquid Mg, compared with those in Al/Al_2O_3 system. The bulk energy difference between <MgO> and {MgO} is about 4.4Jm^{-2}, much higher than that between <Al_2O_3> and {Al_2O_3}. The large bulk energy difference leads to a small h_a^c in the Mg/MgO system.

Fig. 5 shows the dependence of h_a^c on T. h_a^c decreases with increase of T in the temperature range of 650 to 1050^{o}C. h_a^c is about 0.15nm at 650^{o}C, i.e. less than 1ML, suggesting that the amorphous oxide phase is thermodynamically unstable above T_m.

3.3 Ga/Ga_2O_3

The β-Ga_2O_3 {100} crystallographic plane has the lowest energy,[26] and was chosen for the < β-Ga_2O_3 > overgrowth on the surface of liquid Ga, competed with {Ga_2O_3} overgrowth. Fig. 6 shows bulk, interfacial and surface energy differences, as well as the corresponding total Gibbs energy difference of the amorphous oxide overgrowth and the corresponding crystalline oxide overgrowth on the surface of liquid Ga for h_a=1.0nm at 29^{o}C. The contribution of negative energy term is also governed by the corresponding interfacial energy difference between γ_a^i and γ_c^i. Fig. 7 shows the dependence of h_a^c on temperature. It can be seen that h_a^c is almost independent of T in the temperature range of 29-327^{o}C. h_a^c is about 0.35nm, i.e. 2MLs, at 29^{o}C, indicating that the amorphous oxide phase is thermodynamically preferred in the considered temperature range.

4. Discussion

Only a few experimental observations on the initial oxide overgrowth at free surface of liquid metals have been reported,[8,9,32] due to the difficulty in experimental operation. It was reported that a monolayer of amorphous Al_2O_3 film can be formed in the initial oxidation of liquid Al at oxygen partial pressure of 3×10^{-3}Torr.[8] The prediction, according to the thermodynamic model calculation in the liquid Al-Al_2O_3 system, revealed that the critical thickness of thermodynamically stable amorphous phase is 6-8MLs in the temperature range of 650~1050^{o}C. Therefore, the formation of an amorphous oxide monolayer is thermodynamically preferred in the initial oxidation of liquid Al. For the liquid Ga-Ga_2O_3 system, the calculated critical thickness of an amorphous oxide film is about 0.35nm in the temperature range of 27-327^{o}C. The experimental observation confirmed that an amorphous Ga_2O_3 film with a thickness of 0.5nm formed in the temperature range from room temperature to 300^{o}C and on the oxygen partial pressure of 1.8×10^{-4}~1.6×10^{-3}Torr.[9] It should be noted that the accuracy of the parameters used in the model calculation can affect the reliability of the predicted results to a certain extent. Given the errors in both the thermodynamic model calculation and the experimental observation, the predictions agree well with the experimental results. By contrast, for the liquid Mg-MgO system the predicted critical thickness of an amorphous oxide film is less than 1ML in the temperature range of 650~1050^{o}C, i.e. the amorphous oxide phase is thermodynamically unstable in the initial oxidation of liquid Mg. No experimental observation on the structure of oxide film in the initial oxidation of liquid Mg had been reported, partially due to the very high evaporation pressure of Mg. However, oxidation of liquid Mg usually produces a discontinuous oxide film on the surface.[7] In the initial oxidation on a bare solid Mg, the predicted critical oxide-film thickness, up to which the amorphous {MgO} overgrowth is thermodynamically preferred, is below 1ML for all Mg substrate orientations,[13] as confirmed by the experimental observation.[33,34] It implied that the prediction of the initial oxide overgrowth at the free surface of liquid Mg seemed to be acceptable.

Both the experimental observations and model predictions are indicative of the formation of an amorphous oxide film in the initial oxidation on liquid Al and Ga. In the Al and Ga oxide systems, the bulk energy difference between the amorphous and crystalline oxides is relatively small, and then the negative energy contribution from surface and interfacial energy difference can compensate the positive energy contribution for the bulk term. The energy balance of negative surface and interfacial terms and positive bulk term produce a thermodynamically stable amorphous phase up to a few MLs near T_m. However, the bulk energy difference is quite large for the Mg oxide systems, compared to that of the Al and Ga oxide systems. As a consequence, the positive energy term can't be compensated by the sum of surface and interfacial energy terms in at least 1ML of MgO oxide film, resulting in thermodynamic instability of the amorphous phase.

Different from the initial oxide overgrowth on a bare solid metal surface,[13,14] the strain energy and dislocation contributions between the crystalline oxide and metal substrate are absent in the interfacial energy term between the crystalline oxide and LM for the initial oxidation of LMs. In the initial oxide overgrowth on a bare solid metal surface, the strain and dislocation energies are positive energy terms and contribute to the thermodynamic stability of amorphous oxide overgrowth. However, the calculated sum of strain and dislocation energy contributions is relatively small and does not exceed the value of $0.5 Jm^{-2}$ for all metal/oxide systems studied in the literature.[14] The decrease in the bulk Gibbs energy difference between the amorphous and crystalline oxide phases with increasing growth temperature is also preferred to the thermodynamic stability of amorphous phase in the initial oxidation for both at the free surface of LMs and on a bare solid metal surface. In both cases, the temperature dependence of h_a^c is governed by the decrease in the bulk Gibbs energy difference. It is noted that h_a^c in the initial oxidation of liquid Al exhibits the same positive temperature dependence as that in the initial oxide overgrowth on the solid Al surfaces.[13] The predicted h_a^c in the initial oxidation on liquid Al is about 1.3nm at 700^oC, much larger than that in the initial oxidation on solid Al, about 0.6nm at 298^oC. It is suggested that the amorphous oxide phase formed during the oxidation on the solid Al can be further stabilized with an increase of temperature beyond T_m. Therefore, the amorphous phase observed in the initial oxidation at the free surface of liquid Al in the literature[8] is indeed thermodynamically preferred.

5. Summary

Based on the thermodynamic model for the oxide overgrowth on the solid metal surface developed recently by Mittemeijer and co-workers, we have developed a thermodynamic model to analyze the thermodynamic stability of oxide overgrowth on liquid metals. In the Al/Al_2O_3 and Ga/Ga_2O_3 systems, the thermodynamic model predictions revealed that the positive bulk Gibbs energy difference between amorphous and crystalline oxides can be compensated for up to a critical thickness of a few atomic layers by the negative energy difference of surface and interfacial terms, and thermodynamically stabilizes the amorphous oxide phase. However, the bulk Gibbs energy difference is relatively large for the Mg/MgO system, and can't be compensated for by the surface and interfacial energy difference. The critical thickness of thermodynamically preferred amorphous phase is about 1.3nm for the $Al/\gamma\text{-}Al_2O_3$ and 0.33nm for the $Ga/\ \beta\text{-}Ga_2O_3$ system, respectively, at the melting point of the LMs. The amorphous oxide is thermodynamically unstable for the Mg/MgO system.

Acknowledgements

Financial support under grant EP/H026177/1 from the EPSRC is gratefully acknowledged.

References:

1. M. Merkwitz and W. Hoyer: *Z. Metallkd.*, 1999, 90, 363-370.
2. D. Giuranno, E. Ricci, E. Arato and P. Costa: *Acta Mater*., 2006,54,2625-2630.
3. J. M. Molina, R. Voytovych, E. Louis and N. Eustathopoulos: *Int. J. Adhes. Adhes*., 2007, 27, 394-401.
4. B. M. Gallois: *JOM Journal of the Minerals, Metals and Materials Society*, 1997, 49, 48-51.
5. H. Fujii, S. Izutani, T. Matsumoto, S. Kiguchi and K. Nogi: *Mater. Sci. Engi. A*, 2006, 417, 99-103.
6. S. A. Impey, D. J. Stephenson and J. R. Nicholls: *Mater. Sci. Technol.*, 1988, 4, 1126-1132.
7. S. P. Cashion, N. J. Ricketts and P. C. Hayes: *J. Light Metals*, 2002, 2, 43-47.
8. F. Stucki, M. Erbudak and G. Kostorz: *Appl. Surf. Sci.*, 1987, 27, 393-400.
9. M. J. Regan, H. Tostmann, P.S. Pershan, O. M. Magnussen, E. DiMasi, B. M. Ocko and M. Deutsch: *Phys. Rev. B*, 1997, 55, 10786-10790.
10. K. R. Lawless: *Rep. Prog. Phys.*, 1974, 37, 231-316.
11. L. P. H. Jeurgens, W. G. Sloof, F. D. Tichelaar and E. J. Mittemeijer: *J. Appl. Phys.*, 2002, 92, 1649-1656.
12. L. P. H. Jeurgens, A. Lyapin and E. J. Mittemeijer: *Acta. Mater.*, 2005, 53, 4871-4879.
13. L.P.H.Jeurgens, W. G. Sloof, F. D. Tichelaar and E. J. Mittemeijer: *Phys. Rev. B*, 2000, 62, 4707-4719.
14. F. Reichel, L. P. H. Jeurgens and E. J. Mittemeijer: *Acta. Mater*., 2008, 56, 659-674.
15. K. Shinohara, T. Seo and H. Kyogoku: *Z. Metallkd*., 1982, 73, 774-780.
16. M. W. Chase Jr.: in 'NIST-JANAF thermochemical tables', 4th edn, 59-1539; 1998, J. Phys. Chem., Ref. Data.
17. W. J. Bernard and J. W. Cook: *J. Electrochem. Soc*., 1959, 106, 643-646.
18. A. Leu, S. Ma, and H. Eyring: *Proc. Nat. Acad. Sci. USA*, 1975, 72, 1026-1030.
19. D. B. Dingwell: *J. Am. Ceram. Soc*., 1992, 75, 1656-1657.
20. Y. S. Touloukian, R. K. Kirby, R. E. Taylor and T. Y. R. Lee: 'Thermal expansion: Nonmetallic solids, Thermophysical properties of matter', Vol.13, 2-200; 1977, New York, IFI/Plenum.
21. H. Yanagida and G. Yamaguchi: *Bull. Chem. Soc. Jpn*., 1964, 37, 1229-1231.
22. N. Ikemiya, J. Umemoto, S. Hara and K.Ogino: *ISIJ Int.*, 1993, 33, 156-165.
23. S. Blonski and S. H. Garofalini: *Surf. Sci.*, 1993, 295, 263-274.
24. J. J. Gilman: *J. Appl. Phys*., 1960, 31, 2208-2218.
25. G. Jura and C. W. Garland: *J. Am. Chem. Soc.*, 1952, 74, 6033-6034.
26. V. M. Bermudez: *Chem. Phys.*, 2006, 323, 193-203.
27. N. Zouvelou, D. Skarmoutsos and P. Nikolopoulos: *Key Eng. Mater.*, 2004, 679, 264-268.
28. R. C. Weast: 'Handbook of chemistry and physics', 55th edn, 22-31; 1974, CRC, Ohio.
29. W. Hoyer, I. Kaban and M. Merkwitz: *J. Opt. Adv. Mater.*, 2003, 5, 1069-1073.

30. G.N. Antonow: *J. Chem. Phys*., 1907, 5, 372-384.
31. T. Iida and R. I. L. Guthrie: 'The physical properties of liquid metals', 133-134; 1988, Oxford, Clarendon.
32. A.J. Bevolo, J. D. Verhoeven and M. Noack: *Surf. Sci.*, 1983, 134, 499-528.
33. L.P.H. Jeurgens, M.S. Vinodh and E. J. Mittemeijer: *Acta*. *Mater*., 2008, 56, 4621-4634.
34. M. Kurth, P. C. J. Graat, H. D. Carstanjen and E. J. Mittemeijer: *Surf. Interface Anal.*, 2006, 38, 931-940.

Table 1 Physical data of the Al/Al_2O_3, Mg/MgO and Ga/Ga_2O_3 (T_0=298°C).

Surface	Symbol	Value	Unit	Ref.
		Molar volumes at T_0		
$\{Al_2O_3\}$	V_a^o	3.19×10^{-5}	m^3mole^{-1}	17
$<\gamma\text{-}Al_2O_3>$	V_c^o	2.81×10^{-5}	m^3mole^{-1}	17
{MgO}	V_a^o	5.42×10^{-5}	m^3mole^{-1}	18
<MgO>	V_c^o	1.10×10^{-5}	m^3mole^{-1}	18
$\{Ga_2O_3\}$	V_a^o	3.81×10^{-5}	m^3mole^{-1}	19
$<\beta\text{-}Ga_2O_3>$	V_c^o	3.19×10^{-5}	m^3mole^{-1}	19
		Coefficients of linear thermal expansion $\alpha(T)=a+b\cdot\Delta T$		
$<\gamma\text{-}Al_2O_3>$	a	2.068×10^{-6}	K^{-1}	21
	b	1.1499×10^{-8}	K^{-2}	21
<MgO>	a	11.0×10^{-6}	K^{-1}	18
	b	6.0×10^{-10}	K^{-2}	18
$<\beta\text{-}Ga_2O_3>$	a	-2.0×10^{-6}	K^{-1}	29
	b	0	K^{-2}	29
		Surface energies at T_m		
$<\gamma\text{-}Al_2O_3>\{111\}$	γ_c^m	0.94	Jm^{-2}	23
<MgO>	γ_c^m	2.53	Jm^{-2}	24, 25
$<\beta\text{-}Ga_2O_3>\{100\}$	γ_c^m	1.13	Jm^{-2}	26
liquid Al	γ_{LM}^m	0.914	Jm^{-2}	31
liquid Mg	γ_{LM}^m	0.559	Jm^{-2}	31
liquid Ga	γ_{LM}^m	0.718	Jm^{-2}	31
		Temperature coefficient of surface energies		
$\{Al_2O_3\}$	$\partial\gamma_a^s/\partial T$	-0.187×10^{-3}	$Jm^{-2}k^{-1}$	22
$<\gamma\text{-}Al_2O_3>$	$\partial\gamma_c^s/\partial T$	-0.5×10^{-3}	$Jm^{-2}k^{-1}$	14
{MgO}	$\partial\gamma_a^s/\partial T$	0.07×10^{-3}	$Jm^{-2}k^{-1}$	14
<MgO>	$\partial\gamma_c^s/\partial T$	-0.476×10^{-3}	$Jm^{-2}k^{-1}$	27
$\{Ga_2O_3\}$	$\partial\gamma_a^s/\partial T$	0.04×10^{-3}	$Jm^{-2}k^{-1}$	14
$<\beta\text{-}Ga_2O_3>$	$\partial\gamma_c^s/\partial T$	-0.4×10^{-3}	$Jm^{-2}k^{-1}$	14
liquid Al	$\partial\gamma_{LM}^s/\partial T$	-0.35×10^{-3}	$Jm^{-2}k^{-1}$	31
liquid Mg	$\partial\gamma_{LM}^s/\partial T$	-0.35×10^{-3}	$Jm^{-2}k^{-1}$	31
liquid Ga	$\partial\gamma_{LM}^s/\partial T$	-0.10×10^{-3}	$Jm^{-2}k^{-1}$	31

Figure captions:

Fig. 1 Schematic drawing of a homogeneous M_xO_y oxide film with uniform thickness on the surface of liquid metals (*LM*s). (a) An amorphous oxide film $\{M_xO_y\}$ with thickness of h_a; (b) A crystalline oxide $<M_xO_y>$ film with a thickness of h_c (the braces {} refer to the amorphous phase, and the brackets <> to the crystalline phase). Amorphous cell $h_a \times l_a^2$ in (a) and crystalline cell $h_c \times l_c^2$ in (b) have the same composition, formed from the same molar quantity of oxygen on the surface of an identical *LM*.

Fig. 2 Bulk (ΔG^b), interfacial ($\Delta\gamma^i$) and surface energy ($\Delta\gamma^s$) differences, as well as the corresponding total Gibbs energy difference ($\Delta G^t=\Delta G^b+\Delta\gamma^s+\Delta\gamma^i$), as functions of oxide-film thickness (h_a) for the amorphous oxide $\{Al_2O_3\}$ overgrowth and the corresponding crystalline $<\gamma\text{-}Al_2O_3>$ oxide overgrowth on the surface of liquid Al at a growth temperature of 700°C. The positive ΔG^b increases with h_a, however the sum of negative $\Delta\gamma^s$ and $\Delta\gamma^i$ terms is independent of h_a. The critical thickness h_a^c is determined by the point at $\Delta G^t=0$. h_a^c is about 1.3nm at 700°C (as indicated by the arrow).

Fig. 3 Temperature dependence of critical thickness h_a^c for the amorphous $\{Al_2O_3\}$ oxide overgrowth in the initial oxidation on liquid Al. On the surface of liquid Al, the amorphous oxide overgrowth was competed with the crystalline $<\gamma\text{-}Al_2O_3>$ oxide overgrowth with {111} crystallographic plane as the terminated surface. h_a^c is 1.28nm at 660°C, and increases slightly with T. Below h_a^c, an amorphous oxide film is thermodynamically preferred than a crystalline film.

Fig. 4 ΔG^b, $\Delta\gamma^i$, $\Delta\gamma^s$ and ΔG^t as functions of h_a for the amorphous oxide $\{MgO\}$ overgrowth and the corresponding crystalline $<MgO>$ oxide overgrowth on the surface of liquid Mg at a growth temperature of 700°C. The positive ΔG^b term increases rapidly with h_a, and leads to the thermodynamic instability of the amorphous phase. The relatively large ΔG^b suppresses the critical thickness up to h_a^c=0.15nm.

Fig. 5 Temperature dependence of h_a^c for the amorphous $\{MgO\}$ oxide overgrowth in the initial oxidation on liquid Mg. h_a^c is 0.15nm at 650°C, and decreases further with T. h_a^c is less than 1ML at 650°C, suggesting that an amorphous oxide film is thermodynamically unstable in the considered temperature range. A crystalline <MgO> oxide film instead of an amorphous oxide film is thermodynamically preferred on the surface of liquid Mg.

Fig. 6 ΔG^b, $\Delta\gamma^i$, $\Delta\gamma^s$ and ΔG^t as functions of h_a for the amorphous oxide $\{Ga_2O_3\}$ overgrowth and the corresponding crystalline $<\beta\text{-}Ga_2O_3>$ oxide overgrowth on the surface of liquid Ga at a growth temperature of 29°C. The positive ΔG^b term can be compensated up to h_a^c of 0.35nm at 29°C (as indicated by the arrow) by the sum of negative $\Delta\gamma^s$ and $\Delta\gamma^i$ terms.

Fig. 7 Temperature dependence of h_a^c for the amorphous $\{Ga_2O_3\}$ oxide overgrowth in the initial oxidation on liquid Ga. On the surface of liquid Ga, the amorphous oxide overgrowth was competed with the crystalline $<\beta\text{-}Ga_2O_3>$ oxide overgrowth. The calculated h_a^c is nearly independent of T in the considered temperature range. h_a^c=0.35nm (about 2MLs) at 29^{o}C, indicating that an amorphous $\{Ga_2O_3\}$ oxide overgrowth instead of a crystalline oxide overgrowth is thermodynamically preferred.

Fig1(a)

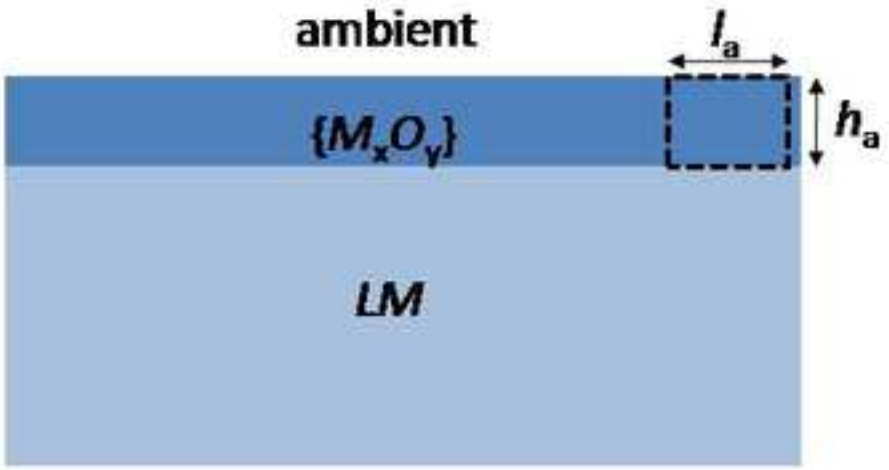

(a) amorphous $\{M_xO_y\}$

Fig1(b)

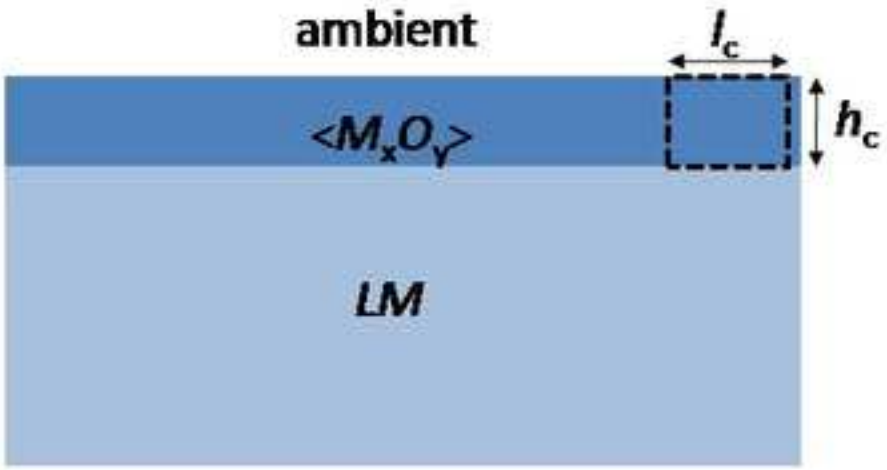

(b) crystalline $<M_xO_Y>$

Fig2

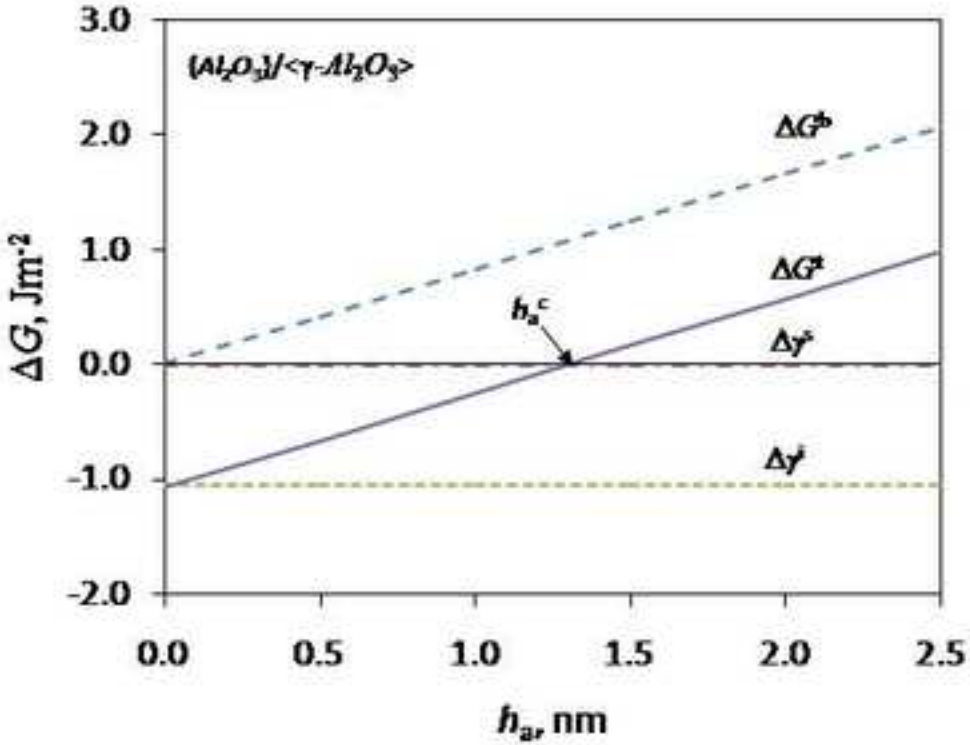
(Al2O3)/<γ-Al2O3>
ΔG*b
ΔG*
h_a^c
Δγ^c
Δγ^i
ΔG, Jm-2
h_a, nm
3.0
2.0
1.0
0.0
-1.0
-2.0
0.0
0.5
1.0
1.5
2.0
2.5

Fig3

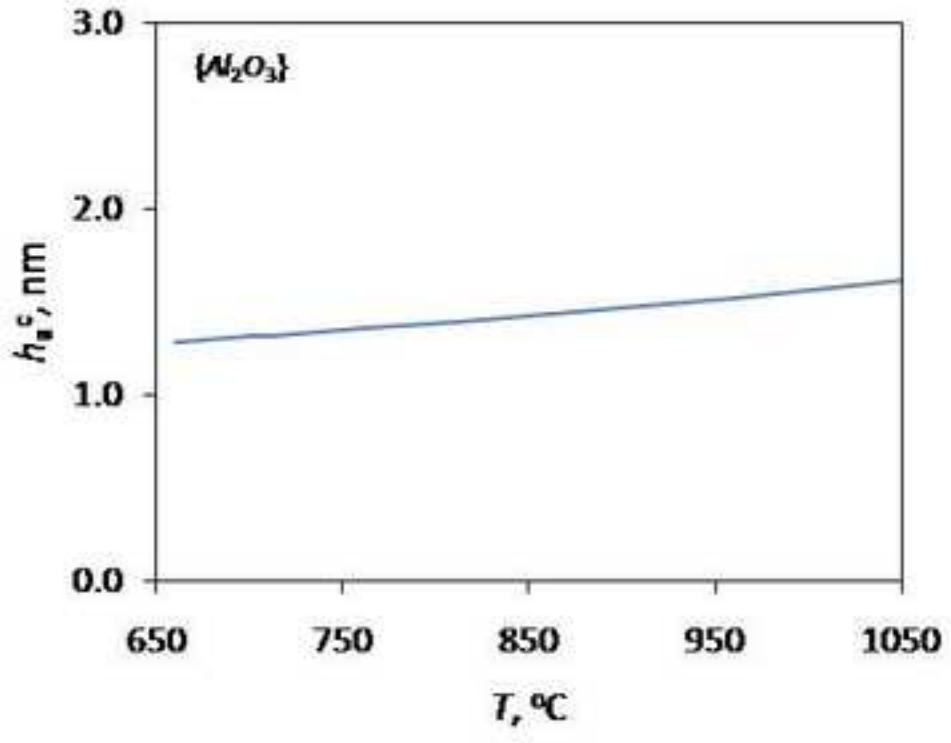

Fig4

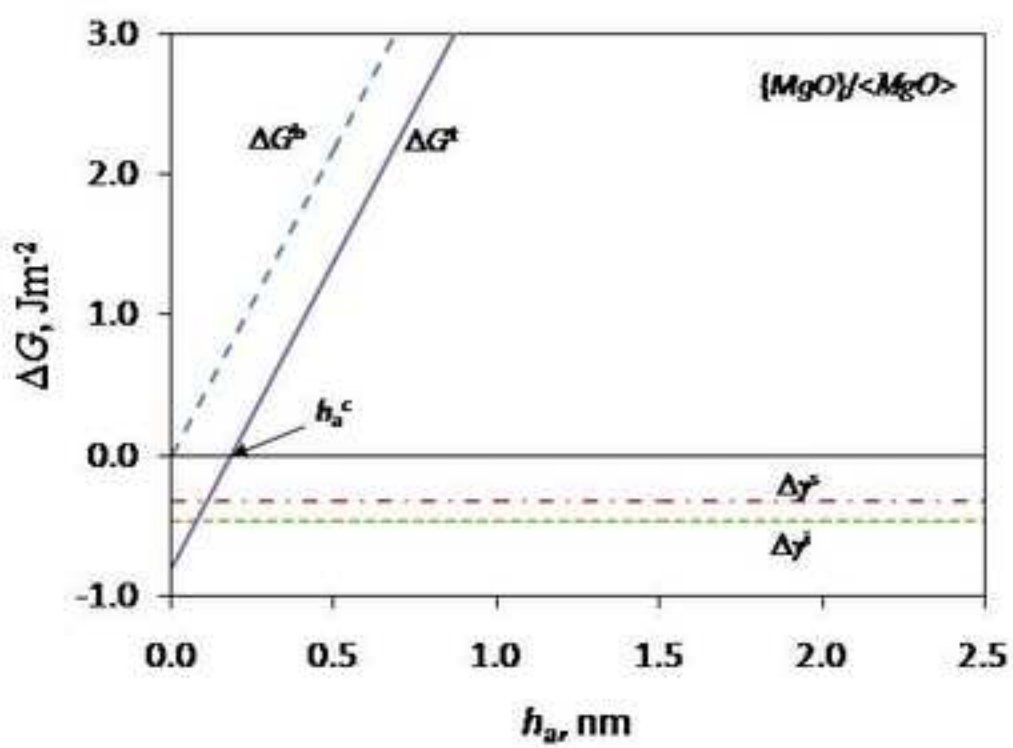
3.0
2.0
1.0
0.0
-1.0
0.0
0.5
1.0
1.5
2.0
2.5
ΔG, Jm-2
ha, nm
{MgO}/<MgO>
ΔGb
ΔGt
hac
Δγs
Δγi

Fig5

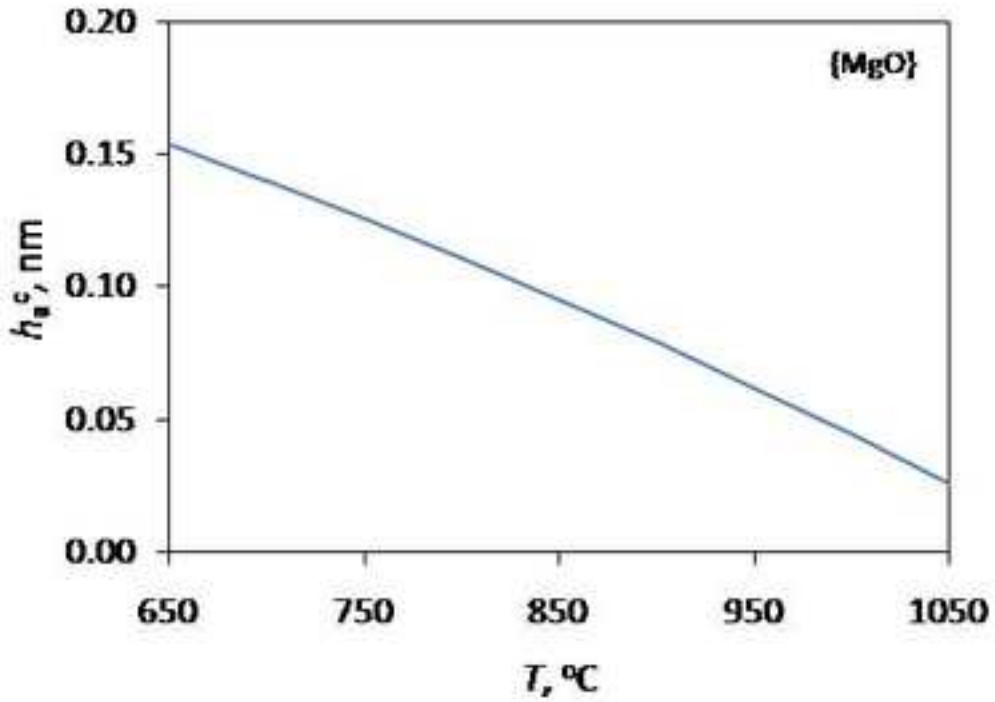

Fig6

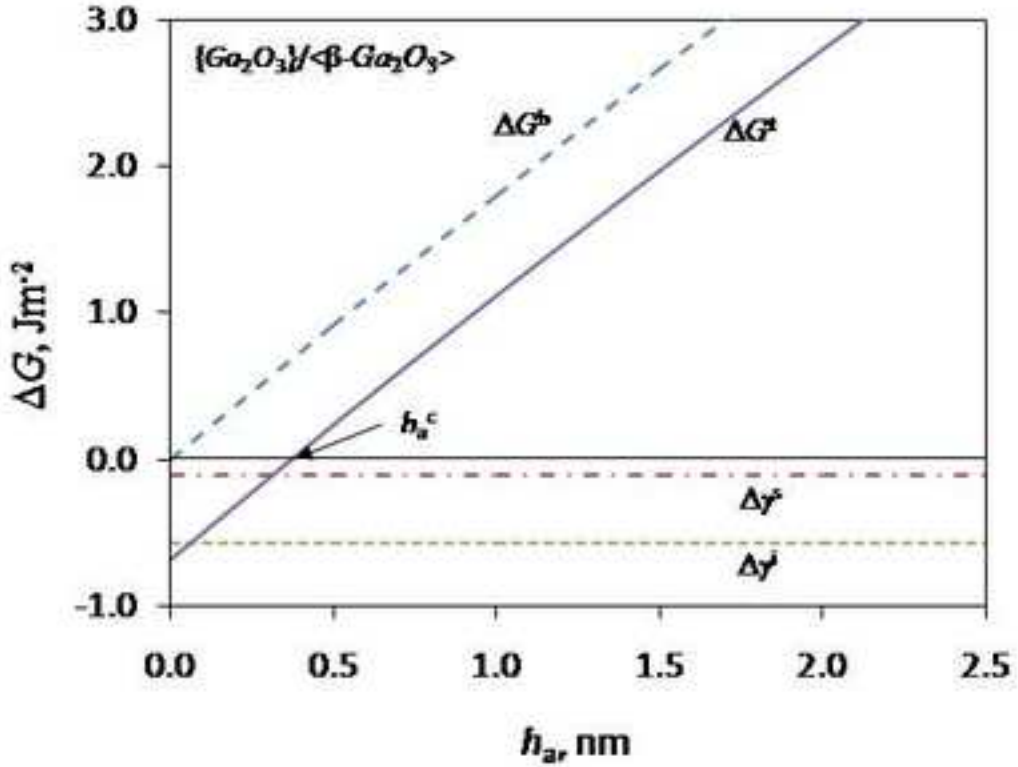
{Ga2O3}/<β-Ga2O3>
ΔG^b
ΔG^a
h_a^c
Δγ^a
Δγ^b
ΔG, Jm^-2
h_a, nm
3.0
2.0
1.0
0.0
-1.0
0.0
0.5
1.0
1.5
2.0
2.5

Fig7